TOWARDS SIMULATION OF ELECTROMAGNETICS AND BEAM PHYSICS AT THE PETASCALE*

Z. Li[1], V. Akcelik, A. Candel, S. Chen, L. Ge, A. Kabel, L.-Q. Lee, C. Ng, E. Prudencio, G. Schussman, R. Uplenchwar, L. Xiao, K. Ko, SLAC, Menlo Park, CA 94025, USA

Abstract

Under the support of the U.S. DOE SciDAC program, SLAC has been developing a suite of 3D parallel finite-element codes aimed at high-accuracy, high-fidelity electromagnetic and beam physics simulations for the design and optimization of next-generation particle accelerators. Running on the latest supercomputers, these codes have made great strides in advancing the state of the art in applied math and computer science at the petascale that enable the integrated modeling of electromagnetics, self-consistent Particle-In-Cell (PIC) particle dynamics as well as thermal, mechanical, and multi-physics effects. This paper will present 3D results of trapped mode calculations in an ILC cryomodule and the modeling of the ILC Sheet Beam klystron, shape determination of superconducting RF (SCRF) cavities and multipacting studies of SCRF HOM couplers, as well as PIC simulation results of the LCLS RF gun.

INTRODUCTION

High performance computing (HPC) for accelerator modeling and simulation has played an important role in the design and optimization of existing and future accelerators. Under the DOE computational initiative "Scientific Discovery through Advanced Computing" (SciDAC) Accelerator Simulation and Technology (AST) project [1, 2] started in 2001, SLAC has developed a parallel accelerator modeling capability for use on HPC platforms to enable large-scale electromagnetic simulations. Running on DOE flagship supercomputers at NERSC [3] and NCCS [4], the codes developed under SciDAC1 have been applied to improve existing and to design future accelerators across the offices of High Energy Physics (HEP), Basic Energy Sciences (BES) and Nuclear Physics (NP) under the Office of Science (SC).

Under SciDAC2 Community Petascale Project for Aceelerator Science and Simulation (COMPASS), SLAC will continue to enhance its parallel accelerator modeling capability for challenging large-scale simulations on petascale supercomputers. The SLAC activities will be focused in the following areas: parallel code development, collaborations in applied mathematics and computer science (AM/CS), and accelerator applications. For parallel code development, we will extend our current electromagnetic capability to integrate self-consistent PIC particle dynamics and thermal/mechanical multi-physics analysis. To exploit the power of petascale computing, advances in AM/CS are deemed even more desirable than in SciDAC1. We will collaborate with SciDAC CET's/Institutes researchers on the areas of scalable solvers, shape optimization, adaptive refinements and visualization. These concerted efforts will aim at tackling the most challenging problems for various accelerator projects such as simulating the ILC [5] 3-cryomodule RF unit, improving the performance of the SNS [6] cavities, and virtual prototyping of the RIA RF quadrupole including multi-physics effects.

In this paper, we will present the current status of code development and simulation efforts.

PARALLEL CODE DEVELOPMENT

The electromagnetic codes developed at SLAC are based on high-order Parallel Finite Element (PFE) method for geometry fidelity and simulation accuracy. Under SciDAC1, a suite of parallel codes in production mode has been developed and includes:

Omega3P: a complex eigensolver for finding normal modes in resonant structures with open ports, impedance boundaries or lossy materials;

S3P: a frequency domain solver for calculating scattering parameters of RF components;

T3P: a time-domain solver for simulating transient response of RF driven systems and for calculating wakefields due to charged beams;

Track3P: a particle tracking code for calculating dark current and analyzing multipacting in RF cavities and components;

V3D: a visualization tool for fields and particles in unstructured grids.

Under SciDAC2, three new electromagnetic codes and one beam dynamics code will be developed. They are

Gun3P: a space-charge electron trajectory code in static fields for modeling formation and transport of DC beams;

Pic3P: a particle-in-cell code for self-consistent simulation of particle and RF field interactions in RF guns and klystrons;

TEM3P: an integrated multi-physics code including electromagnetic/thermal/mechanical effects for cavity design;

Nimzovich: a 3D strong-strong beam-beam code for beam lifetime calculations.

In the following sections, we will present some of the accelerator R&D problems simulated using these codes.

05 Beam Dynamics and Electromagnetic Fields   D05 Code Developments and Simulation Techniques

HOM DAMPING IN ILC LL CAVITY

The Low-Loss cavity design [7, 8] (Fig. 1) is being considered as a possible upgrade to the baseline TESLA cavity for the ILC main linac. The optimized LL shape has 10% lower B_{peak}/E_{acc} ratio and 15% higher R/Q and geometric factor G than the TESLA design. With the low B_{peak}/E_{acc}, the LL design could support an ultimate gradient of over 50 MV/m as the maximum gradient achievable is believed to be limited by the critical magnetic flux B_c of niobium at 180 mT [9]. The low B_{peak}/E_{acc} ratio leads to 20% reduction in cryogenic loss. The realization of such a high gradient design for the ILC linacs would lead to significant cost saving in machine construction and operation. Properly damping the high R/Q dipole modes is important for beam stability and emittance preservation for the ILC linac. The multipacting in the end-group needs to be alleviated in order to achieve a high gradient.

The end-group of the LL design is optimized using Omega3P [10] for HOM damping. A high fidelity mesh consisting of 0.53M quadratic elements (3.5M DOFs) was used to model the cavity. This provides sufficient resolution for modifying the end-groups to improve the HOM damping. By adjusting the end-pipe radius, the HOM coupler azimuthal location, and the loop shape and configuration (see Fig. 1), the Qe of the dangerous 3rd band mode was reduced to below the stability threshold of 1×10^5 as shown in Fig. 2. The multipacting in the end-group was simulated using Track3P. The geometries of the coupler were optimized to fully suppress multipacting barriers within the gradient range of ILC.
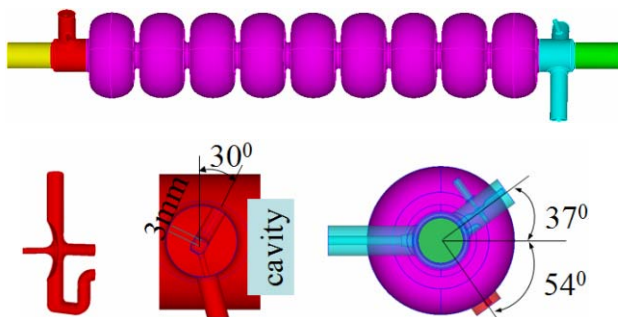

Figure 1: The optimized end-groups of the LL shape cavity for effective HOM damping.
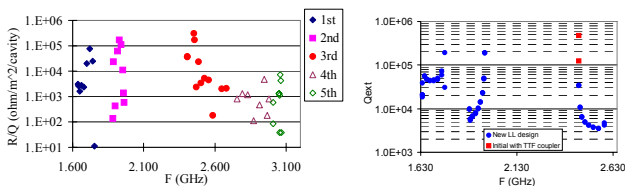

Figure 2: Dipole mode R/Q and damping results of the LL cavity using Omega3P.

ILC TDR CAVITY IMPERFECTION STUDY

The manufacturing process, the tuning and the handling of the superconducting cavities may introduce deformations to the designed shape. The effects of these deformations have been observed in the measured data of the TTF cryomodules. In the 9-cell TDR cavity, each dipole band consists of 9 pairs of modes. The degeneracy of the pairs is split by 3D effects of the couplers. With cavity imperfection, the frequencies and Q factors of different cavities scatter and shift from the ideal cavity. Fig. 3 shows the frequencies and Qe's of the 6th pair in the second dipole band of the 8 cavities in a TTF module. The two black dots are the Omega3P results for the ideal cavity. Compared with the ideal case, the splitting of the measured mode pairs is larger, the mode pair mostly shifts to lower frequencies, and the Qe's scatter mostly toward high values. The Qe increase would be problematic if their values exceed the beam stability limit. The large frequency split of the mode pair is the result of perturbation to the field distribution by the imperfection, which may induce x-y coupling and dilute the beam emittance.
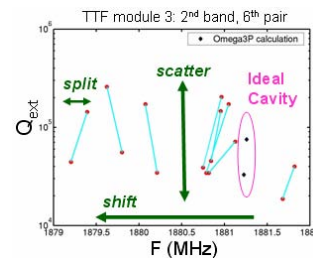

Figure 3: Scatter in measured dipole mode data in TTF cavities.
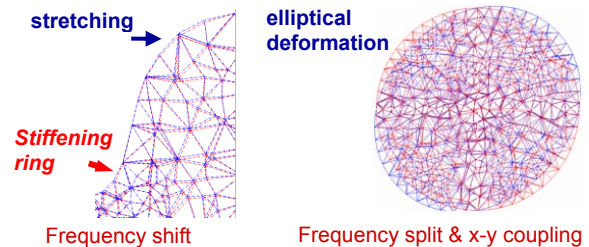

Figure 4: (Left) Deformed cell surfaces that cause frequency shift; (Right) Elliptical cell deformation that causes frequency split as well as x-y coupling.

Understanding the tolerance requirements on cavity imperfection is important for the ILC cavity development. However, the imperfection of the cavity is not well understood because of the complicated procedure and steps involved in cavity manufacturing and treatment. In order to model realistic cavities for the ILC beam dynamics study, we have embarked on an effort to determine the true cavity shape by solving an inverse problem [11, 12], using the data from the TESLA data bank [13] as input parameters. Progress has been made in identifying key imperfection parameters that cause the discrepancy between the measured data and the Omega3P calculation of an ideal cavity. Fig. 4 shows some possible cavity deformations identified through the shape determination process. Fig. 5 shows the polarizations of the 6th dipole pair in the 2nd dipole band for the ideal cavity and a deformed cavity with elliptical cells. It can be seen that the polarizations of the dipole pair are quite

different for the two cases, and their changes in the deformed cavity could lead to the enhancement of x-y coupling for wakefield effects. These deformation parameters will be used to produce realistic cavities for beam dynamics studies of the ILC linac.
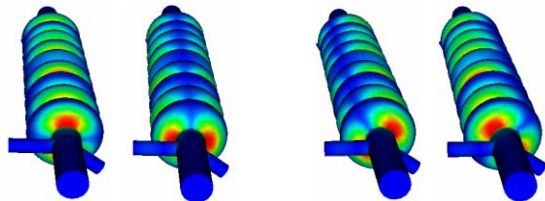

Figure 5: Field patterns of a dipole pair in (Left) ideal cavity; (Right) cavity with elliptical cells.
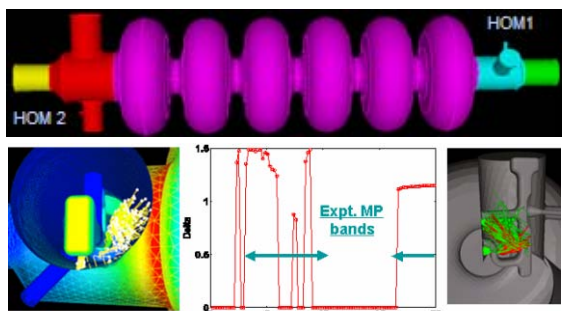
MULTIPACTING IN SNS BETA=0.81 CAVITY

Figure 6: Multipacting in the SNS HOM coupler.

During the commissioning and operation of the SNS superconducting linac, abnormal signals were observed at the HOM coupler [14]. These anomalies are believed to be due to the field emission and multipacting electron loadings in the HOM coupler. To understand these issues, the field enhancement and multipacting were simulated using Omega3P and Track3P. Fig. 6 shows the model of the SNS beta=0.81 cavity. The fundamental coupler is located at the upstream beampipe, and two HOM couplers are at opposite sides of the cavity. The upstream beampipe has a larger radius for more efficient FM coupling. As a result, the field in the upstream coupler region is much larger than that in the downstream. At the field gradient of 16 MV/m, the field strength in the notch gap of HOM2 (upstream) is about 14 MV/m and that in HOM1 (downstream) about 3 MV/m. The high field gradient in the HOM2 could cause field emission and multipacting. Multipacting analysis using Track3P shows two multipacting bands in the gradient range up to 20 MV/m. One of the multipacting bands exists in the gap between the enlarged loop head and the cylindrical side wall of the coupler at field gradient levels from 2.8 to 10 MV/m as shown on the left of Fig. 6. The other MP band exists in the gap between the hook part of the loop and the cylindrical side wall of the coupler as shown on the right of Fig. 6. No MP activities are found in the notch gap. These MP bands are in good agreement with the experimental observations [15].

MULTIPACTING ANALYSIS FOR TTF-III COUPLER

The TTF-III coupler [16] (Fig. 7) adopted for the ILC baseline cavity design has shown a tendency to have long initial high power processing times. A possible cause for the long processing times is believed to be multipacting in various regions of the coupler. To understand performance limitations during high power processing, SLAC has built a flexible high-power coupler test stand [17]. The plan is to test individual sections of the coupler using the test stand to identify problematic regions. To provide insights to the high power test results, detailed numerical simulations of multipacting for these sections have been carried out using Track3P. Fig. 7 shows a model of the "cold" coax in the high power test. In addition to monitoring the vacuum pressure, an electron pickup is placed on the outside wall of the coax to measure the electron activities. The calculated MP bands as well as the measured pickup signal and the vacuum current after initial processing showing in Fig. 8 exhibit good agreement between simulations and measurements [17, 18].
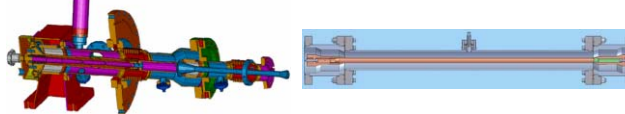

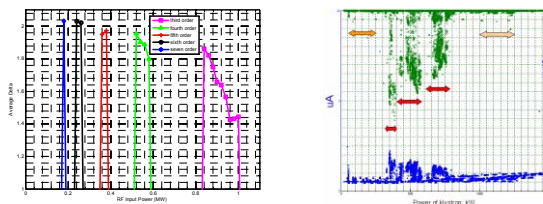Figure 7: (Left) the TTF-III coupler; (Right) cold coax test setup.

Figure 8: (Left) MP bands from Track3P simulation and (Right) high power measurement data of the cold coax.

Other coupler components including the cold/warm bellows and the cold window are being simulated. Simulation results will be used for high power test studies and possible coupler modifications to reduce the processing time during high power processing.

PARALLEL FE PARTICLE CODES

Currently two particle codes, Gun3P and Pic2P/3P, are being developed for simulating self-consistent charged particle beam formation and transportation in RF circuits such as high power klystrons and RF guns. These codes are based on finite element unstructured grids and are designed to run on distributed memory computers. Taking advantage of the large memory and computing power of parallel computers, these codes allow unprecedented high resolution analysis of beams in complex and large problem geometry with fast turnaround time. There are growing interests to use these self-consistent beam codes to simulate large systems such as the entire LCLS RF

05 Beam Dynamics and Electromagnetic Fields

D05 Code Developments and Simulation Techniques

photo-injector and the ILC sheet beam klystron (SBK) from end to end, which will allow system scale optimization for beam quality and RF efficiency.

Gun3P: One of the target applications for Gun3P is the DC gun for the SBK [19]. The SBK is presently being developed at SLAC for the ILC as an alternative high power RF source. Because of the elongated elliptical beam transverse profile, the problem is fully 3-dimensional. Currently available codes for modeling DC guns run on single CPU machines. The size of the problem and the amount of design details that can be modeled using these codes are limited by the memory and runtime of single processor. Gun3P overcomes these limitations by using high-order finite elements and parallel processing for accuracy and speed. The standard ingredients required for a gun code such as the space-charge limited cathode emission model, an electro- and a magneto- static solver for calculating the space charge field and the self-magnetic field, and self-consistent particle tracking have been implemented. Fig. 9 shows the electron trajectories in the ILC L-band SBK DC gun with an anode voltage of 115 kV using Gun3P. The evaluation of the self-magnetic field of the beam stick is required to obtain the correct trajectories. The right plot in Fig. 9 shows the runtime reduction as a function of the number of processors. The parallel capability of Gun3P will facilitate the convergence study for the SBK gun design.
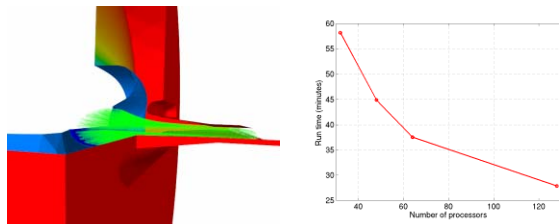

Figure 9: (Left) Electron trajectories in the ILC L-band SBK gun cavity with 115 kV anode voltage, as computed by Gun3P. Also shown is the electric potential on the cavity walls; (Right) Gun3P runtime versus number of processors.

Pic2P/3P: The Particle-In-Cell (PIC) method is a commonly used approach for self-consistent simulation of electromagnetic field and charged particle interaction. Most PIC codes are formulated on the orthogonal finite-difference grid because the implementation is straightforward, although some have succeeded with non-orthogonal grids to provide better geometry accuracy. We have completed a parallel implementation of the PIC method on a 2D unstructured grid with quadratic conformal elements and adaptive refinement of the basis function order (up to 6th), resulting in a highly efficient code (Pic2P). In benchmark runs for the LCLS RF gun design [20] (Fig. 10), Pic2P exhibits excellent agreement with MAFIA, while converging much faster, requiring two orders of magnitude fewer field unknowns and less than ten CPU minutes. PARMELA results differ as soon as space-charge and wakefield effects are important (Fig. 11) (for more details, see [21]). Studies of PIC

simulations in long structures as well as the extension to 3D (Pic3P) are underway. When completed, Pic3P will provide a new design tool for simulating the LCLS photo-injector including the effects of laser pulse non-uniformity. It can also be used for the study of beam-field interactions in the ILC L-band sheet-beam klystron.
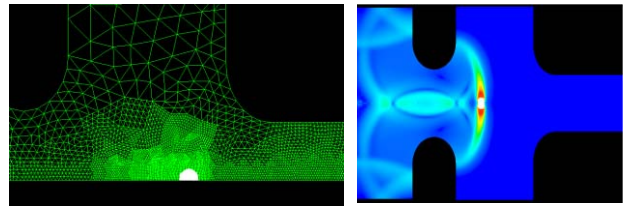

Figure 10: (Left) Triangular elements in the LCLS gun mesh with adaptive *p*-refinement, (Right) snapshot in time of charged bunch shown with fields in the LCLS gun cavity.
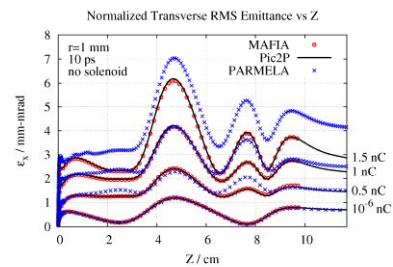

Figure 11: Comparison of the emittance of the LCLS RF gun using Pic2P, MAFIA and PARMELA (see text for details).

PARALLEL STRONG-STRONG BEAM-BEAM SIMULATION

We have developed a set of codes [22] for the simulation of beam-beam effects in storage ring colliders. The two codes, NIMZOVICH and PLIBB have been originally developed for different uses. The former is a strong-strong code, using particle-in-cell (PIC) methods to self-consistently track particles in lepton machine to establish equilibrium luminosities. It has now been optimized for the case of many parasitic crossings and head-on-collisions requiring high longitudinal resolution, as they occur in designs with pronounced hourglass effect. PLIBB was designed to go beyond obtaining quantities like tune footprints and dynamic aperture available as simulation results from traditional tracking codes. By using highly-optimized tracking algorithms and massive parallelization, the code is able to calculate actual loss rates for hadron colliders under the influence of nonlinear elements, including the weak-strong beam-beam interaction which is modeled analytically using a fast approximation of the complex error functions.

PLIBB has been augmented with full tracking-code functionalities, including element-by-element tracking capabilities and differential-algebraic methods. It is able to read MAD-X lattice definitions and has been extensively benchmarked against MAD-X. The strong-strong algorithms of NIMZOVICH have been implemented into PLIBB, making integrated simulations of machines such as the LHC feasible. We are currently

05 Beam Dynamics and Electromagnetic Fields

D05 Code Developments and Simulation Techniques

benchmarking the code against dedicated beam-beam and wire-compensator experiments carried out at RHIC. Fig. 12 demonstrates the high loss-rate resolution calculation of a loss-rate versus beam separation scan for a RHIC lattice with a single parasitic crossing. It shows the expected signature of a sudden drop in losses when increasing the distance beyond six sigmas.
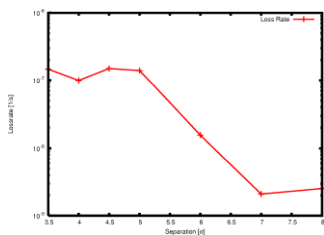

Figure 12: High-resolution loss rate calculation for RHIC loss rate vsersus beam separation.

ILC CRYOMODULE SIMULATION

An ILC RF unit consists of three cryomodules driven by one klystron, and each cryomodule has 8 or 9 cavities. While HOM damping has been optimized for individual cavities, its effects for modes above the beam-pipe cutoff have not been fully investigated. It is of great interest to understand the trapped modes and their damping in the RF unit with realistic cavity imperfections and misalignments, to study beam heating and the effectiveness of beamline absorbers in the interconnects between cavities and cryomodules. Successful simulations of this large system would provide invaluable information on issues that are important to the machine performance, enabling system validation in the R&D phase. As a first step toward this goal, the first-ever calculation of dipole modes in a cryomodule has been successfully performed on the NERSC supercomputer. A typical mode in the 3rd dipole band is shown in Fig. 13. One can see that the polarization of the mode rotates through the cryomodule. The effects could induce significant x-y coupling to beam dynamics, which need to be understood and minimized. The effectiveness of HOM couplers on damping these modes is determined by the field patterns in the interconnects, and will be strongly affected by cavity imperfections and misalignments. These issues will be best addressed through simulating the multi-cavity system.
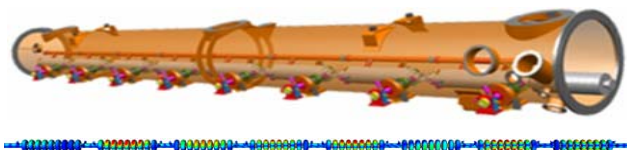

Figure 13: ILC 8-cavity TTF cryomodule and a HOM mode in the 8 -cavity module from Omega3P**.**

In simulating the eight-cavity cryomodule on NERSC Seaborg, the runtime was 1 hour per mode using 300 GB of memory on 1024 CPUs for the problem size with 20 million DOFs. It is estimated that 200 million DOFs would be required to simulate the ILC 3-cryomodule RF unit. Petascale computing resources together with advances in computational science research will definitely be needed in achieving this goal. In fact, in order to successfully simulate the above cryomodule on current supercomputers, a new memory reduction scheme was developed for the parallel linear solver that enables to solve problems twice as large with the same available memory [23].

ACKNOWLEDGMENTS

REFERENCES

[1] http://www.scidac.gov/.
[2] K. Ko et.al., SciDAC and the International Linear Collider: Petascale Computing for Terascale Acelerator, Proc. SciDAC 2006 Conference, Denver, Colorado, June 25-29, 2006.
[3] http://www.nersc.gov.
[4] http://nccs.gov.
[5] http://www.linearcollider.org.
[6] http://neutrons.ornl.gov.
[7] J. Sekutowicz et al., JLAB, TN-02-023, June 2002.
[8] Z. Li et al., "Optimization of the Low Loss SRF Cavity For the ILC", these proceedings.
[9] K. Saito, "Fundamental RF critical Field Overview", Proc. Workshop on Pushing the Limits of RF Superconductivity, ANL, Argonne, September 2004.
[10] L. Lee et al., "Modeling RF Cavity with External Coupling", 2005 SIAM Conference on Computational Science and Engineering, Orlando, Florida, 2005.
[11] V.Akcelik et.al., "Adjoint Methods for Electroma- gnetic Shape Optimization of the Low-Loss Cavity for the International Linear Collider", Proc. SciDAC 2005, San Francisco, California, 2005.
[12] L. Xiao et al., "Modeling imperfection effects on dipole modes in TESLA cavity", these proceedings.
[13] G. Kreps, private communications.
[14] S.-H. Kim, et al., "Study on Fault Scenarios of Coaxial Type HOM Couplers in SRF Cavities", Proc. LINAC2006, Knoxville, 2006.
[15] S.-H. Kim, private communications.
[16] http://tesla-new.desy.de
[17] Brian Rusnak, et al., "High-Power Coupler Component Test Stand Status and Results", these proceedings.
[18] L. Ge, et al., "Multipacting Simulations of TTF-III Coupler Components", these proceedings.
[19] A. Burke, private communications.
[20] L. Xiao et.al., Dual Feed RF Gun Design for the LCLS, Proc. PAC 2005, Knoxville, Tennessee, May 15-20, 2005.
[21] A. Candel et al., "Parallel Higher-order Finite Element Method for Accurate Field Computations in Wakefield and PIC Simulations", Proc. ICAP06, Chamonix Mont-Blanc, 2006, & these proceedings.
[22] A. Kabel, et al., "Recent Progress in Beam-Beam Simulation Codes", these proceedings.
[23] L.-Q. Lee et al., "Enabling Technologies for Petascale Electromagnetic Simulations", Proc. SciDAC 2007, Boston, Massachusetts.

05 Beam Dynamics and Electromagnetic Fields

D05 Code Developments and Simulation Techniques